3D-Printed ABS plastic Peanut-Lens with Integrated Ball Grid Array-Module for High-Data Rate Communications in F-band

Journal:	*IET Microwaves, Antennas & Propagation*
Manuscript ID	MAP-SI-2017-0190.R1
Manuscript Type:	Research Paper
Date Submitted by the Author:	24-Jul-2017
Complete List of Authors:	Bisognin, Aimeric; Université de Nice-Sophia Antipolis, EPIB Arboleya, Ana; Universidad de Oviedo, Electrical Engineering, Area Teoria de la Señal y Comunicaciones LUXEY, Cyril; University Nice Sophia-Antipolis, EPIB; Institut Universitaire de France, IUF Gianesello, Frederic; ST Microelectronics, T R&D, TPS Lab Gloria, Daniel; STMicroelectronics France, Matos, Sergio; Instituto de Telecomunicacoes Carlos, Jorge; Instituto de Telecomunicacoes Fernandes, Carlos; Instituto Superior Técnico, Instituto de Telecomunica鉄es
Keyword:	DIELECTRIC MATERIALS, MILLIMETRE WAVE ANTENNAS, PRINTED ANTENNAS, ANTENNA RADIATION PATTERNS, ANTENNA MEASUREMENTS, ANTENNAS IN PACKAGE, LENS ANTENNAS

3D-Printed ABS plastic Peanut-Lens with Integrated Ball Grid Array-Module for High-Data Rate Communications in F-band

Aimeric Bisognin [1,2], Ana Arboleya [1], Cyril Luxey [1*], Frederic Gianesello [2], Daniel Gloria [2], Sérgio A. Matos [3,4], Jorge R. Costa [3,4], Carlos A. Fernandes [4]

[1] Polytech'Lab, University Nice Côte d'Azur, Campus Sophia-Tech, France
[2] STMicroelectronics, Crolles, France
[3] DCTI, Instituto Universitário de Lisboa (ISCTE-IUL), Lisbon, Portugal
[4] Instituto de Telecomunicações, Instituto Superior Técnico, Lisbon, Portugal

[*] cyril.luxey@unice.fr

Abstract: A ball grid array (BGA) module integrated within a 3D-printed Peanut-Shaped lens is proposed for high data-rate wireless communications in the F-band (116 GHz- 140 GHz) between a video camera and a TV or a laptop. The module implements a 1×2 array antenna which radiates a wide beam in the horizontal plane (H-plane) and a narrower beam in the vertical plane (E-plane). The dielectric lens, fabricated in ABS-M30 plastic, is a shaped lens designed to achieve a fan-beam radiation pattern further narrowing the vertical plane and widening the horizontal plane of the BGA module. The realized gain of the full antenna-system is required to exceed 5 dBi within a 120º angular interval in the horizontal plane and a 20º angular interval in the vertical plane. Measurements show a reflection coefficient below -9 dB from 116 to 140 GHz and a maximum realized gain of 8.5 dBi at 130 GHz demonstrating feasibility of the cost-effective proposed design for a high-data rate communications.

1. Introduction

Due to the constant improvement in wireless communications and the demand of each time higher data rates, a huge research effort has been done during the last years to develop communication systems at high frequency bands that can cope with requirements regarding not only high-data rates but also compactness and cost-effective manufacturing processes to address the consumer market.

New communication standards such as the WiGig IEEE 802.ad have become very popular within last years due to the multi-gigabit throughput, up to 7Gbps [1], that can be achieved in the broadband unlicensed frequency V-band around 60 GHz. Several commercial chipsets [2-4] as well as fully integrated antenna packages [5-7] have been developed at 60 GHz enabling a wide variety of applications in the consumer electronics industry ranging from media streaming docking stations [8-10] to wireless virtual reality applications [11]. However, considering the fact that data rates up to 10 Gbps might be soon required [12], millimetre-wave (mm-wave) bands above 100 GHz are the perfect compromise for those high-data rate requirements while still meeting the required miniaturization for a good integration of the communication systems within the wireless devices [13].

The free-licensed part of the F-band ranging from 116 GHz to 142 GHz provides a very large frequency bandwidth and thus, it has become a very appealing option for multi-gigabit data rate wireless communications [12-16].

Due to this large available bandwidth in the F-band, the spectral requirements can be relaxed allowing for the use of more energy efficient modulation schemes such as On-Off Keying (OOK) schemes. Besides, high propagation and wall penetration losses, make this band a perfect candidate for line-of-sight (LoS) in-room wireless personal area communications (WPAN). Hot-topic applications include wireless ultra-high-definition video/audio transmission from a 4K video camera to a TV or laptop in a framework similar to the one described in ***Fig. 1***.

For a LoS communication of 3 m in the F-band as the one described in ***Fig. 1*****,** and considering the radio performance of a typical transceiver with OOK modulation [17,18], 5dBi gain antennas are needed at both sides of the wireless link (typical values of 18 dBm transmitted power and -50 dBm sensitivity have been used for the link budget calculation).

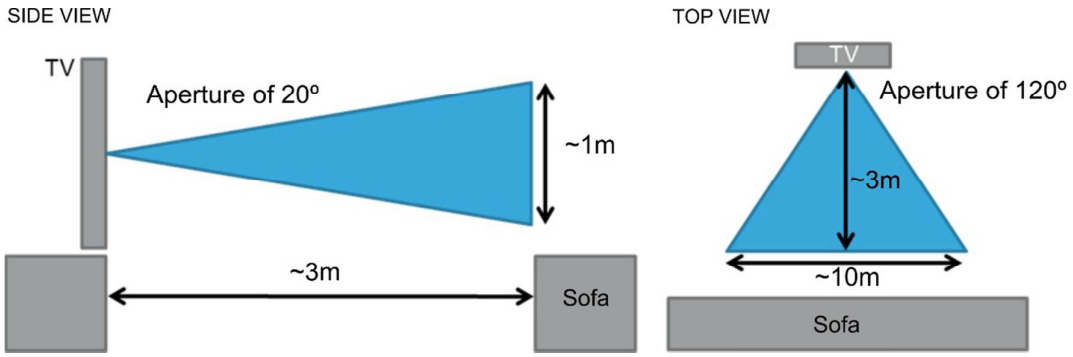

Fig. 1. *Framework of the application for the use of the BGA module integrated within a shaped lens with wide aperture in the horizontal plane and focalized beam in the vertical plane.*

Three dimensional (3D) shaped lenses are convenient solutions for achieving a fan radiated beam by transforming the radiation pattern of the ball grid array (BGA) module to meet the aperture requirements given in ***Fig. 1***. Furthermore, the low-cost ABS-M30 plastic widely employed in phone manufacturing and communication devices housing, and the cost-effective manufacturing technology known as fusing deposition modelling (FDM) are the ideal choices not only in terms of size and performance, but also in terms of cost for the consumer target we focus on.

In this paper, a BGA antenna-module integrated within a plastic lens is proposed for high data-rate wireless communications in the F-band in the scenario presented in ***Fig. 1***. The antenna design is described in detail in Section 2, focusing on the BGA technology, the 1×2 array antenna source for the

dielectric lens and then, the design and the fabrication of the peanut-shaped lens itself. Measurement results of the full antenna system are presented in Section 3 demonstrating promising results for the developed cost-effective solution. Finally, main conclusions are drawn in Section 4.

2. Antenna design

In order to cope with the abovementioned requirements regarding the distance and position of the transmitter and receiver devices, a cost-effective lens fabricated in ABS-M30 plastic has been conjointly designed with a 1 x 2 antenna array source integrated in a BGA module to radiate a fan beam. The realized gain is required to exceed 5 dBi within a 120º angular interval in the horizontal plane (H-plane, or XZ-plane in ***Fig. 3***) and 20º angular interval in the vertical plane (E-plane or YZ-plane in ***Fig. 3***) giving the user a good margin to place the video camera device anywhere within the sofa without compromising the data link (See ***Fig. 1***).

Before designing the lens, a printed antenna should be developed to feed the lens from its base. This configuration with the feed embedded in the lens is usually designated by integrated lens antenna [19] and it is much more compact than the common approach of having an external feed illuminating the lens surface.

2.1. BGA Module

Standard high density interconnect (HDI) technology has been employed for the development of the BGA. This technology allows for minimum trace resolution and minimum spacing of 50 μm. A standard 1-2-1 build-up with core thickness of 200 μm and prepreg layers of 30 μm, enabling four metallization layers, has been chosen. The three-substrate layers have been made from the same substrate of relative permittivity $\varepsilon_r = 3.4 - j0.01$. A schematic view of the layers and elements distribution is shown in ***Fig. 2***.

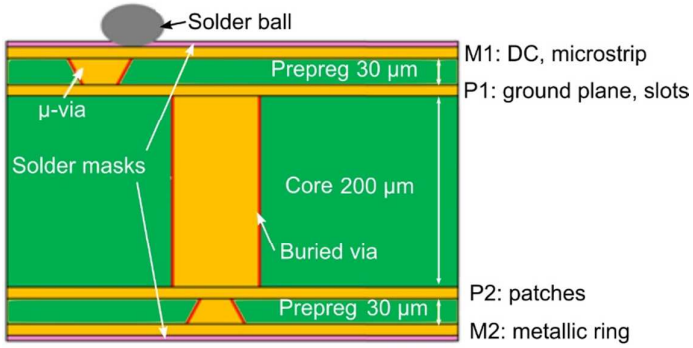

Fig. 2. *Distribution of the layers and possible vias in the 1-2-1 BGA build-up.*

The BGA module design is shown in transparent view in ***Fig. 3*** a. The pad ring of the chip is seen in the left side of the figure and will be further connected to the BGA in flip-chip by means of copper pilar technology. Solder balls will be employed to connect the BGA to the printed circuit board (PCB). An antenna array is integrated in the BGA, radiating in the opposite direction of the chip, in order to minimise the radiation over the chip. The main dimensions of the BGA module are $7 \times 7 \times 0.362$ mm^3.

A detailed view of the 1×2 antenna array is shown in ***Fig. 3*** b. Each radiating element is linearly polarized and is formed by an aperture-coupled patch, the apertures being excited through a microstrip line underneath them in order to maximize the matching and gain bandwidth. The microstrip line implements a 1 : 2 power divider which distributes the power equally between both patches.

As shown in ***Fig. 3*** b, the antennas are arranged on the y-axis with 1 mm separation between them ($0.43\lambda_0$ at 130 GHz, central frequency of the band). Thus, a wide beam is expected for the XZ-plane while in the YZ-plane the beam should be focused, as required to illuminate the lens. A metallic cavity has also been included around the patches in order to collect the residual energy due to the TM_0 surface modes and reradiate it in phase with the main beam.

A photograph of the top and bottom layers of the fabricated BGA is shown in ***Fig. 3.*** The chip, the DC pads and the microstrip power divider in layer M1 can be clearly observed in ***Fig. 3*** c, while ***Fig. 3*** d shows the bottom layer, M2, with the cavity and a dummy pad (necessary for metal density balance). The antenna patches in layer P2 can be also seen through the transparent prepreg substrate.

The antenna array has been optimized to radiate in ABS-M30 plastic, the material that will be used to manufacture the lens. Simulations of the 1×2 array have been carried out with HFSS [20] considering the BGA is surrounded by an ABS-30 medium for $z > 0$.

The reflection coefficient remains below -9 dB from 92 GHz to 140 GHz. The different loops in the locus of the imput impedance, shown in ***Fig. 4*****,** indicate good matching of the designed BGA source.

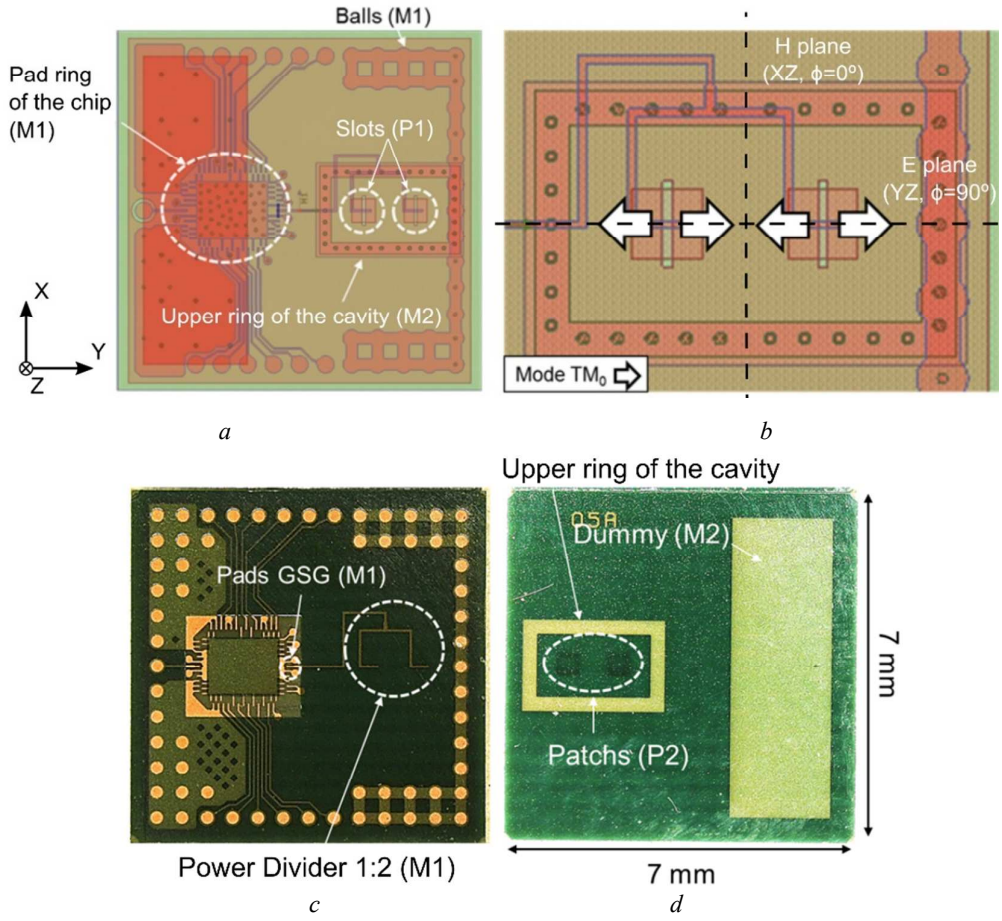

Fig. 3. *BGA module.*
a Top transparent view
b Bottom transparent view (zoom on patch antennas only)
c Top view of the manufactured prototype
d Bottom view of the manufactured prototype

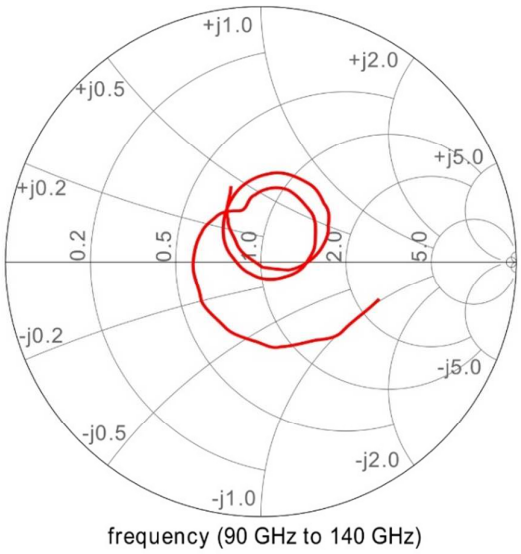

Fig. 4. *Simulation results of the input impedance of the 1×2 antenna array radiating in an ABS-M30 plastic infinite medium.*

The simulated main cuts of the normalized radiation patterns of the 1 × 2 antenna array are depicted in ***Fig. 5*** at 120 GHz, 130 GHz and 140 GHz. For the H-plane pattern, the beamwidth at -10 dB is wider than 280º for all the studied frequencies. A beamwidth of approximately 90º is obtained in the E-plane for the 130 GHz and 140 GHz patterns. The asymmetry observed for the 120 GHz pattern (red line in ***Fig. 5*** b) is due to a small misalignment of the BGA module in the lens cavity (see ***Fig. 7*** c).

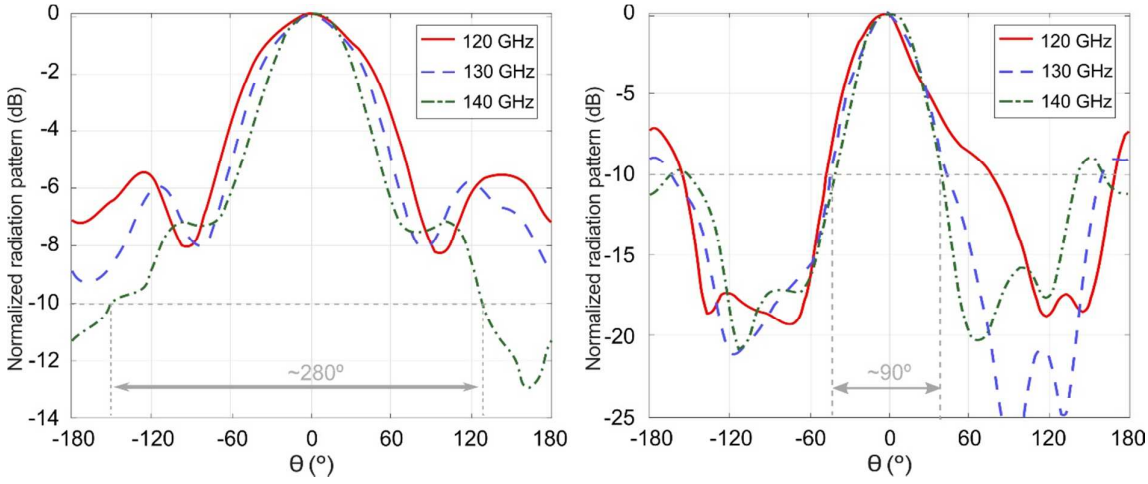

a *b*

Fig. 5. *Simulated normalized radiation pattern of the 1×2 antenna array in an ABS-M30 plastic infinite medium for different frequencies.*

a H plane (ϕ=0º)
b E plane (ϕ=90º)

2.2. Lens

The procedure to design the lens is similar to the one presented in [21]. The first step is to determine the electromagnetic properties of the lens material at the desired working frequencies. Permittivity of the ABS-M30 plastic has been characterized following a procedure described in [22]: $\varepsilon_{r,ABS\,M30} = 2.49 - j0.027$ in the 110 GHz to 125 GHz band. The obtained value is in concordance with values obtained for this material with the setup described in [23]. It is expected and assumed that this value stays constant within the 115-140 GHz frequency interval.

In the second design step, the profile of the lens surface along the horizontal plane (XZ) is determined using the Geometric Optics (GO) formulation implemented in the ILASH software tool [24]. This step requires to use the radiation pattern of the feed array in the horizontal plane (H-plane), presented in ***Fig. 5*** a, and use as target a lens radiation pattern with a flat-top shape with a full beamwidth roll-off of 120º as identified in the application specification in ***Fig. 1*** b. The obtained horizontal cut (XZ) of the lens profile is presented in ***Fig. 6*** a. The figure includes the ray tracing and shows a dispersion of the rays at the top of the lens with parts of the feed radiation being deflected closer to the edges of the lens. This way it is possible for the lens to widen the array radiation pattern into the desired 120º full-width at half maximum (FWHM).

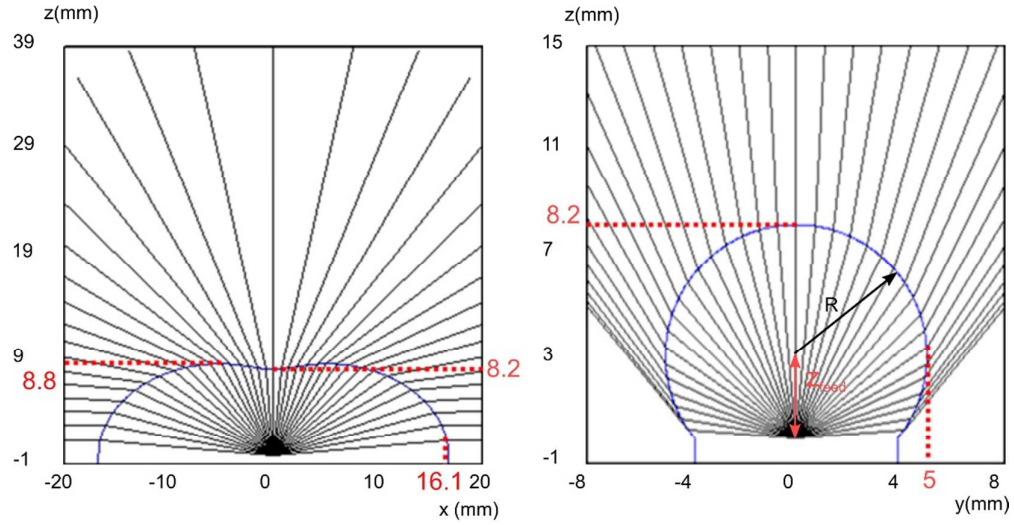

a *b*

Fig. 6. *Geometric profiles and ray tracing analysis for the designed lens.*

a Plane XZ (H-plane)
b Plane YZ (E-plane)

The following design step is to obtain the vertical cut plane (YZ) lens profile. The chosen profile is a circumference with the feed placed below the circumference center at a distance z_{feed}. This profile

corresponds to a 2D cut of a hyper-hemispheric lens [25]. In this lens type the feed distance from the center of the lens is:

$$z_{feed} = R/\sqrt{Re(\varepsilon_{r,ABS\ M30})} \quad (1)$$

where R is the lens radius. In our case the value of R=5 mm is determined so that $R+z_{feed}$ is equal to the height of the lens in the horizontal profiles (XZ) at x=0. The hyper-hemispheric lens tends to focus the radiation from the feed as can be observed from the ray tracing of the lens vertical cut plane (YZ) in ***Fig. 6*** b. This way it is possible to narrow the array vertical plane (E-plane), presented in ***Fig. 5*** b, into the desired application specification in ***Fig. 1*** a of a 20º full beamwidth.

The last design step is devoted to obtain the 3D surface of the lens. To do that, the lens horizontal profile, ***Fig. 6*** a, is rotated along the axis passing in the center of the vertical profile, ***Fig. 6*** b. That is, the axis of rotation is the line (x, y = 0, z = z_{feed}). Total dimensions of the 3D lens are Δx = 32 mm, Δy = 10 mm and Δz = 8.8 mm. Section views of the final prototype are shown in ***Fig. 7*** a and b while the complete design together with a support platform with a cavity to house the BGA feed module, is shown in ***Fig. 7*** c.

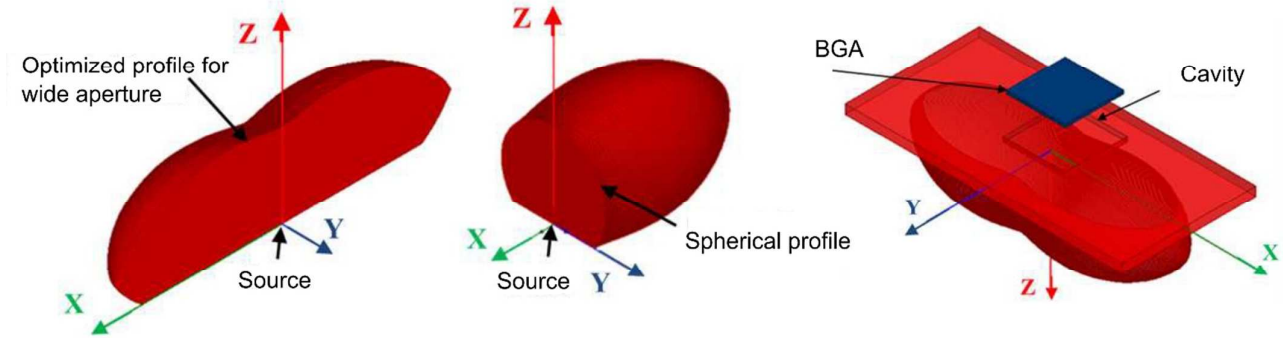

a *b* *c*

Fig. 7. *View of the main cuts of the HFSS lens model.*

a Optimized geometric profile for the plane ZX
b Optimized geometric profile for the plane ZY
c Lens model with the support frame and the cavity for housing the BGA module.

As mentioned before, the lens has been fabricated in ABS-M30 by means of FDM printing technology. ***Fig. 8*** shows the printed lens which looks like a peanut and the BGA module designed as a feed source.

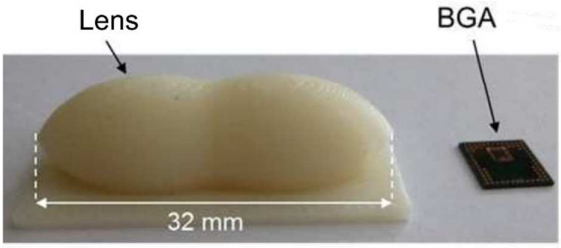

Fig. 8. *Picture of the Final 3D-printed lens prototype with BGA module.*

3. Measurements

Finally, the main parameters of the BGA module with lens have been characterized by means of measurements. The measurement system [26] is composed of a PNA N5247A vector network analyser employed as source, with a VDI N9029AV08 frequency extension module for the F-band, and a HP8563E spectrum analyser, employed to register the field amplitude. The antenna under test (AUT) is fed by means of microelectronic probing, in particular a standard ground-signal-ground (GSG) air to coplanar probe with 150 µm pitch from Cascade-Microtech (ACP140-GSG-150) has been employed. A standard gain horn antenna (Flann SGH 28240-20) is used as the receiving probe. The signal is down converted directly after reception by means of a harmonic mixer (MOHWD WR8) and a rotary joint is installed in the robotic arm in order to minimize errors due to cable flexing in the reception stage. The movement range of the robotic arms is limited by the table on which the system is installed being ~~the angular acquisition range for this acquisition of $-30º < \theta < 225º$ and $0º < \phi < 360º$~~ not possible to acquire the field in the angular section ranging from $-150º < \theta < -40º$.

First the matching parameters of the BGA module integrated with the lens antenna have been measured and the obtained results are compared to those obtained by means of simulations with HFSS. The reflection coefficient is below -9 dB from 116 GHz to 140 GHz which represents an 18.75% relative bandwidth. The measured and simulated input impedance loci, depicted in ***Fig. 9***, are slightly out of phase.

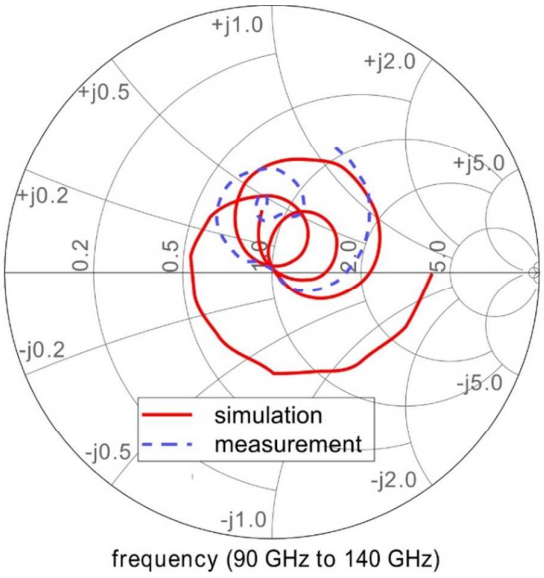

Fig. 9. *Simulated and measured Input impedance of the BGA module integrated within the peanut lens (Simulation ranges from 90 GHz to 150 GHz).*

The realized gain for the main polarization field component along the z-axis (broadside direction) has been measured and compared to the HFSS simulation for the whole F band with very good agreement as depicted in ***Fig. 10***. The realized gain oscillates between 5.5 dBi and 7.5 dBi in the band from 95 GHz to 140 GHz. The measured gain has been approximated by a polynomial interpolation and upper and lower limits considering variations of ±1.2 dB have been depicted in ***Fig. 10*** in order to limit the expected measurement variation due to the uncertainties of the measurement system. As can be seen, except for five frequency points, the rest of measurements lie within the limits and the agreement with simulation results is good. The cross-polar component has also been measured and plotted, showing a polarization purity above 20 dB in the complete F band.

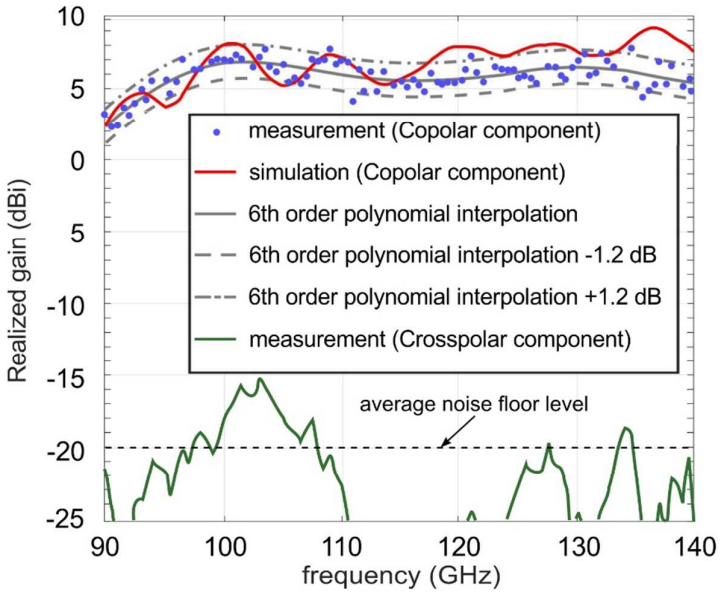

Fig.10 ~~10~~. *Simulated and measured realized gain along the z-axis of the BGA module integrated within the lens for the Co- and Cross-Polarized field components in the F-band.*

Fig. 11 shows the main realized gain cuts at 130 GHz. The agreement between HFSS simulations and measurements is good. A measured beamwidth of 120º at 5dBi gain is obtained in the H-plane versus a 136º aperture obtained from simulations (***Fig. 11*** a). For the E-plane, a beamwidth of 20º at 5 dBi gain is obtained in both cases (***Fig. 11*** b).

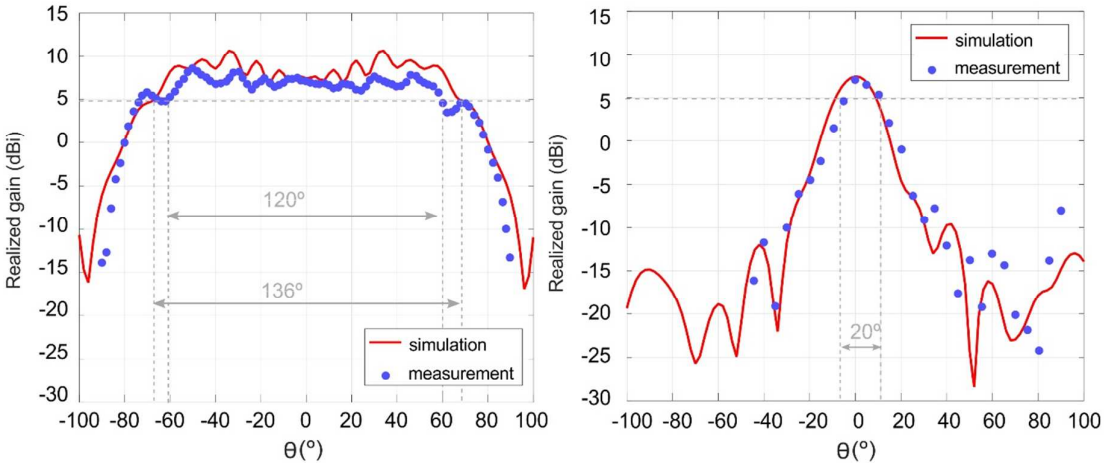

a *b*

Fig. 11~~21~~. *Simulation (blue trace) and measurement (magenta trace) realized gain results of the BGA module integrated within the lens at 130 GHz.*

a H-plane (ϕ=0º)
b E-Plane (ϕ=90º)

The 3D gain patterns at 130 GHz are shown in ***Fig. 12.*** A maximum realized gain of 8.5 dBi is obtained from measurements while the maximum realized gain of the antenna obtained from simulations is 10.7 dBi. This 2 dB difference is probably due to the uncertainties introduced by the test bench together with the masking effect of the probe and the fact that the simulation model did not include the whole BGA source details, and cannot be neglected because a 16º beam reduction is introduced in the horizontal plane of the radiation pattern at 5 dBi gain. Despite this small discrepancy, the observed agreement is still good (note that the back radiation of the measured antenna cannot be recorded due to the mechanical restrictions of the measurement setup) and the antenna prototype meets the initial requirements for the target applications.

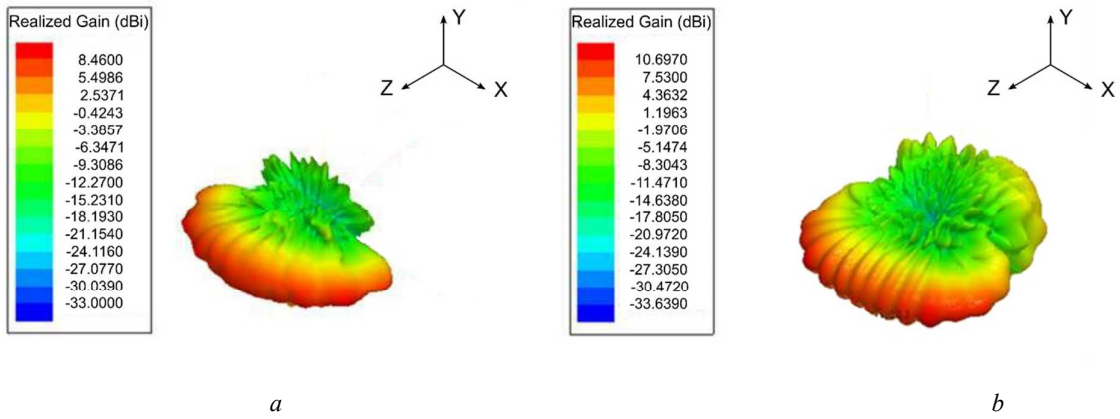

a *b*

Fig. 12. *3D Radiation pattern for the realized gain of the copolar field component at 130 GHz.*

a Measurements partial 3D pattern (*-40º< θ <90º and 0º< ϕ < 360º*)
b Simulation complete 3D pattern

4. Conclusion

In this paper, we presented a proof-of-concept prototype of a cost-effective BGA module integrated within a 3D-printed plastic lens for high data-rate wireless communications between a video camera and a TV or laptop in the F-Band. The BGA module is composed of a 1 × 2 antenna array, and has been conjointly designed with a shaped lens to enhance the gain and to provide a fam beam radiation pattern with at least 120º and 20º at 5 dBi gain in the horizontal and vertical planes respectively, thus the link between the video camera and the TV won't be compromised if small displacements are introduced for any of the two communicating devices.

The antenna array was designed to radiate into ABS-M30 plastic and the lens design is based on Geometric Optics. Full wave electromagnetic simulations of the BGA module and integrated lens have

also been carried out in order to evaluate the complete antenna-prototype behavior. Measurements of the prototype have been performed showing a very good agreement with simulation results in terms of matching and realized gain radiation pattern. The beamwidth requirements at 5 dBi gain are achieved. Variation of the realized gain in the target frequency band (116 GHz – 140 GHz) has also been characterized exhibiting oscillations of less than 1.5 dB. Further work will concentrate on reducing the lens dimensions in order to integrate it within the casing of small communicating devices.

5. References

[1] C. J. Hansen, "WiGiG: Multi-gigabit wireless communications in the 60 GHz band," *IEEE Wireless Communications*, vol. 18, no. 6, pp. 6-7, December 2011.

[2] Peraso "W" series products, Peraso Technologies, online available: http://perasotech.com/w-series-products/ [Accessed 5-March-2017].

[3] Qualcomm Snapdragon 801 processor, online available: https://www.qualcomm.com/products/snapdragon/processors/810, [Accessed 5-March-2017].

[4] Intel wireless Gigabit (802.11ad) products, online available: http://www.intel.com/content/www/us/en/wireless-products/wireless-product-selection-guide.html [Accessed 5-March.-2017].

[5] A. Bisognin, A. Cihangir, C. Luxey, G. Jacquemod, R. Pilard, F. Gianesello, J.R. Costa, C. A. Fernandes, E. B. Lima, C.J. Panagamuwa, W. G. Whittow, "Ball Grid Array-module with integrated shaped lens for WiGig applications in eyewear devices," *IEEE Transactions on Antennas and Propagation*, vol. 64, no. 3, pp. 872-882, March 2016.

[6] H. Mopidevi, H.V. Hunerli, E. Cagatay, B. Biyikli, M. Imbert, J. Romeu, L. Jofre, B.A. Cetiner, "Three-Dimensional Microfabricated Broadband Patch Antenna for WiGig Applications," *IEEE Antennas and Wireless Propagation Letters*, vol. 13, pp. 828-831, 2014.

[7] A. Rahimian, A. Alomainy, Y. Alfadhl, "A flexible printed millimetre-wave beamforming network for WiGig and 5G wireless subsystems," *2016 Loughborough Antennas & Propagation Conference (LAPC)*, Loughborough, pp. 1-5, 2016.

[8] "High-speed 60 GHz wireless connectivity finally takes off," by Digi-Key's European Editors, Digi-Key Electronics, July 2013, online available: https://www.digikey.com/en/articles/techzone/2013/jul/high-speed-60-ghz-wireless-connectivity-finally-takes-off [Accessed 5-March-2017].

[9] HP advanced wireless docking station, online available: http://h20195.www2.hp.com/v2/GetDocument.aspx?docname=4AA6-4497ENW&doctype=data%20sheet&doclang=EN_US&searchquery=&cc=us&lc=en [Accessed 5-March-2017].

[10] Dell wireless docking station, online available: http://www.dell.com/support/article/fr/fr/frbsdt1/SLN297279/the-dell-wireless-docking-station--wld15--wigig-capable-?lang=EN [Accessed 5-March-2017].

[11] Intel's Project Alloy, online available: https://newsroom.intel.com/chip-shots/intel-unveils-project-alloy/ [Accessed 5-March-2015].

[12] J. Wells, "Faster than fiber: The future of multi-G/s wireless," *IEEE Microwave Magazine*, vol. 10, no. 3, pp. 104-112, May 2009.

[13] T.S. Rappaport, F. Gutierrez, "The emerging world of massively broadband devices: 60 GHz and above", Keynote, online available: http://wireless.engineering.nyu.edu/presentations/Keynote_Rappaport.pdf [Accessed 5-March-2017].

[14] C. Wang, C. Lin, Q. Chen, B. Lu, X. Deng and J. Zhang, "A 10-Gbit/s Wireless Communication Link Using 16-QAM Modulation in 140-GHz Band," *IEEE Transactions on Microwave Theory and Techniques*, vol. 61, no. 7, pp. 2737-2746, July 2013.

[15] N. Deferm and P. Reynaert, "A 120 GHz Fully Integrated 10 Gb/s Short-Range Star-QAM Wireless Transmitter With On-Chip Bondwire Antenna in 45 nm Low Power CMOS," *IEEE Journal of Solid-State Circuits*, vol. 49, no. 7, pp. 1606-1616, July 2014.

[16] J. F. Bousquet, "A 10-Gbps energy efficient on-chip wireless communication network for multicore processing", Microelectronics and Solid State Electronics, vol. 3, pp. 9-16, 2014.

[17] Z. Wang, P. Y. Chiang, P. Nazari, C. C. Wang, Z. Chen and P. Heydari, "A CMOS 210-GHz Fundamental Transceiver With OOK Modulation," in IEEE Journal of Solid-State Circuits, vol. 49, no.3, pp. 564-580, March 2014.

[18] N. Dolatsha, B. Grave, M. Sawaby, C. Chen, A. Babveyh, S. Kananian, A. Bisognin, C. Luxey, F. Gianesello, J. Costa, C. Fernandes, A. Arbabian, "A compact 130GHz fully packaged point-to-point wireless system with 3D-printed 26dBi lens antenna achieving 12.5Gb/s at 1.55pJ/b/m", IEEE International Solid-State Circuits Conference (ISSCC 2017), February 2017, San Francisco, USA.

[19] C. A. Fernandes, J. R. Costa, E. B. Lima, and M. G. Silveirinha, "Review of 20 Years of Research on Microwave and Millimeter-wave Lenses at "Instituto de Telecomunicacoes"," *IEEE Antennas and Propagation Magazine*, vol. 57, no. 1, pp. 249-268, March 2015.

[20] ANSYS HFSS, 3D full wave electromagnetic simulator by ANSOFT, online available: "http://www.ansys.com//staticassets/ANSYS/staticassets/resourcelibrary/whitepaper/wp-HFSS-Hybrid-Finite-Element-Integral-Equation-Method.pdf" (retrieved 20th August 2015).

[21] A. Bisognin, A. Cihangir, C. Luxey, G. Jacquemod, R. Pilard, F. Gianesello, et al., "Ball Grid Array-Module With Integrated Shaped Lens for WiGig Applications in Eyewear Devices," *IEEE Transactions on Antennas and Propagation*, vol. 64, no. 3, pp. 872-882, March 2016.

[22] M.G. Silveririnha, C.A. Fernandes, J-R. Costa, "A graphical aid for the complex permittivity measurement at microwave and millimeter wavelengths," *IEEE Microwave and Wireless Components Letters,* vol. 24, no. 6, pp. 421-234, June 2014.

[23] E. Saez, L. Rolo, K. vant Klooser, M. Paquay, V.V. Parishin, "Accuracy assessment of material measurements with a quasi-optical free-space test bench," *European Conference on Antennas and Propagation (EUCAP 2012),* Prague, Czech Republic, pp.149-152, March 2012.

[24] E. Lima, J. R. Costa, M. G. Silveirinha, C. A. Fernandes, "ILASH- Software tool for the design of integrated lens antennas," *IEEE Antennas and Propagation Society International Symposium (AP-S URSI 2008),* San Diego, CA, pp. 1-4, July 2008.

[25] C. A. Fernandes, E. B. Lima, and J. R. Costa, "Dielectric Lens Antennas," in Handbook of Antenna Technologies, Z. N. Chen, Ed., ed Singapore: Springer Singapore, 2016, pp. 1001-1064.

[26] A. Bisognin, D. Titz, F. Ferrero, J. Gilles, R.Pillard, F. Gianesello, D. Gloria, C. Laporte, H. Ezzeldine, D. Lugara , C. Luxey, "Probe-fed measurement system for F-band antennas," *European Conference on Antennas and Propagation (EUCAP 2014),* The Hague, The Netherlands, pp. 722-726, April 2014.

RESPONSE TO THE EDITORS & REVIEWER'S COMMENTS

Paper No.: MAP-SI-2017-0190
Paper Title: 3D-Printed ABS plastic Peanut-Lens with Integrated Ball Grid Array-Module for High-Data Rate Communications in F-band

EDITOR-IN-CHIEF'S COMMENTS

Thank you for submitting your paper to IET Microwaves, Antennas & Propagation. The peer review process is now complete. While finding your paper of relevance and potentially worthy of publication, the associate editor, referees and I feel that significantly more work could be done before the paper can be considered again. My decision is therefore to provisionally accept your paper subject to major revisions.

The referee comments are given below. Please make sure that you have addressed ALL the comments in a detailed covering letter; to be included in both the 'response to decision letter' dialogue box, as well as uploaded as an additional file. Please be aware that your paper may be declined if the changes cannot be easily identified. Please note that if the referees are not convinced that their concerns have been addressed this will, at best, result in a request for further modifications which will delay publication, at worst it could result in rejection. For this reason, when resubmitting your revised manuscript, please deal fully with the reviewers' comments and also explain in the separate document for the reviewers, the changes made and why. If you do not agree with a reviewer's comment you must say so and explain carefully why you do not agree.

ASSOCIATE EDITOR'S COMMENTS

No comments.

Dear Editor-in-Chief, dear Associate Editor, as requested, we considered all the reviewer's comments and we replied to all of them. All the changes are highlighted in the revised version, the parts that have been deleted are crossed-out in red while the parts that have been added to the new version of the manuscript are shown in blue color.

We would like to warmly thank the Reviewers and Editors for their constructive feedback.

REVIEWER 1

1) The authors must give more information about the feed part performance called: "the microelectronic probing".

Author's reply:

The reviewer is right, while the model parts of the source and the receiver are given in the manuscript, no details about the feeding probe are given.

The microelectronic probe employed for feeding the BGA module is a standard F-band GSG (ground-signal-ground) Air-Coplanar Probe from Cascade Microtech, part number ACP140-GSG-150. The probe has 3 tips, 2 for ground and one for signal contacts. The tips are distributed on a constant pitch with approximately 150 microns width. The probe is fed directly with a WR8 waveguide. The part number and main details of the probe have been included in the revised manuscript.

Furthermore, the details of the VDI frequency extension module (N9029AV08), the receiving horn antenna (Flann SGH 28240-20) together with the harmonic mixer (MOHWD WR8) used for downconverting the signal directly at the receiving horn have also been included to completely define the measurement setup RF components.

A more detailed description with pictures can be seen in the provided reference [24]:

A. Bisognin, D. Titz, F. Ferrero, J. Gilles, R.Pillard, F. Gianesello, D. Gloria, C. Laporte, H. Ezzeldine, D. Lugara , C. Luxey, "Probe-fed measurement system for F-band antennas," *European Conference on Antennas and Propagation (EUCAP 2014),* The Hague, The Netherlands, pp. 722-726, April 2014.

The description of the setup has been modified as follows in the revised manuscript:

"Finally, the main parameters of the BGA module with lens have been characterized by means of measurements. The measurement system [24] is composed of a PNA N5247A vector network analyser employed as source, with a VDI N9029AV08 frequency extension module for the F-band, and a HP8563E spectrum analyser, employed to register the field amplitude. The antenna under test (AUT) is fed by means of microelectronic probing, in particular a standard ground-signal-ground (GSG) air to coplanar probe with 150 µm pitch from Cascade-Microtech (ACP140-GSG-150) has been employed. A standard gain horn antenna (Flann SGH 28240-20) is used as the receiving probe. The signal is down converted directly after reception by means of a harmonic mixer (MOHWD WR8) and a rotary joint is installed in the robotic arm in order to minimize errors due to cable flexing in the reception stage. The movement range of the robotic arms is limited by the table on which the system is installed being ~~the angular acquisition range for this acquisition of $-30º < \theta < 225º$ and $0º < \phi < 360º$~~ not possible to acquire the field in the angular section ranging from $-150º < \theta < -40º$."

2) The difference between simulation and measurement is important and the authors didn't explain this difference.

Author's reply:

The differences between simulation and measurements can be attributed to two main causes:

On one hand, the simulation model of the BGA source is not complete since for us it is not possible to perform simulations of the BGA module with all the existing details. In fact, only the antenna elements (and associated feeding network & pads + cavity + vias) have been taken into account in the simulation model. The remaining small details of the BGA module such as the IC DC traces, the large dummy metallic plate, the small metallic square dummies and the ball pads (see Fig. 3 of the revised manuscript) are not taken into account and for sure influence the measurements.

On the other hand, the measurement setup uncertainty, close to ±1.2 dB, and the small beam-depointing of the antenna which can be appreciated in Fig. 11 will introduce some error in the antenna measurement process.

Therefore, some discrepancies are expected between simulation and measurement results. Besides, the electrically-large microelectronic probe that feeds the antenna poses a problem in the characterization of the BGA since the radiation of the probe is expected to modify the real behavior of the antenna. However, the discrepancies have no big impact in the beamwidth at 5 dBi gain, which remains similar for the E-plane and is reduced only 16º for the H-plane.

The following sentence has been added to the reviewed manuscript in order to justify the differences:

"This 2 dB difference is probably due to the uncertainties introduced by the test bench together with the masking effect of the probe and the fact that the simulation model did not include the whole BGA source details, and cannot be neglected because a 16º beam reduction is introduced in the horizontal plane of the radiation pattern at 5 dBi gain."

3) there is no measuring points between -100° and -50° in the E-plane in fig. 11. Why???? especialy the authors gives after in figure 12 the 3D radiation pattern measurement.

Author's reply:

The VDI frequency extension module and the feeding probe are installed on top of a structure which imposes some mechanical restrictions (see figure below), being not possible to acquire the field in the angular section ranging from -150º < θ < -40º. Furthermore, for this measure, only the forward hemisphere has been acquired thus the θ variation is limited from -40º to 90º. The measurement setup description has been slightly modified in the revised manuscript in order to highlight the fact that the field cannot be acquired in the complete sphere due to mechanical descriptions, please check previous answer to see the modifications introduced in the manuscript.

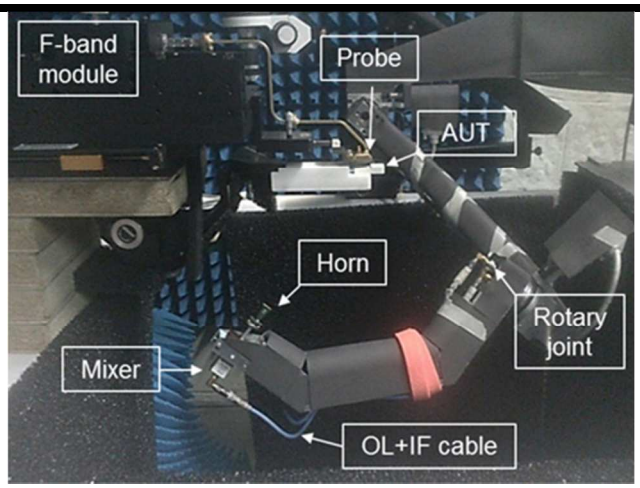

Figure 1. Measurement setup.

Regarding the 3D representation shown in Figure 12, only the simulation results show the complete 3D pattern while for the measurements, the partial 3D pattern with θ varying from -40 to 90 degrees is shown, notice that back radiation of the measurement pattern is not plotted for the measurements (see answer to next question for further explanations).

4) In figure 12. the simulated radiation pattern have a high back radiation level due probably to the back slot radiations. In the same figure, the measured 3D radiation pattern have a very low level, why???The authors must added explanations and comments.

Author's reply:

As mentioned in answers 1 and 2, the mechanical restrictions imposed in the measurement setup don't allow for a full 3D acquisition. In the 3D plot shown in Fig. 12, only the simulations are shown for a complete sphere, while the measurements are shown for the main hemisphere with θ varying from -40 to 90 degrees. The adopted point of view in the plots, which is the one that better shows the front part of the pattern shows data with [0< θ<180] for simulations and with [0< θ<90] for measurements.

Thus, for the measurements the angular margin of [90< θ<180] is not shown in the representation because it cannot be measured, while for the simulations, the complete 3D pattern is shown. In order to clarify this, the angular margin shown in the plots has been added to Figure 12 sub-titles. Also, the following sentence has been added in the revised manuscript:

"Despite this small discrepancy, the observed agreement is still good (note that the back radiation of the measured antenna cannot be recorded due to the mechanical restrictions of the measurement setup) and the antenna prototype meets the initial requirements for the target applications."

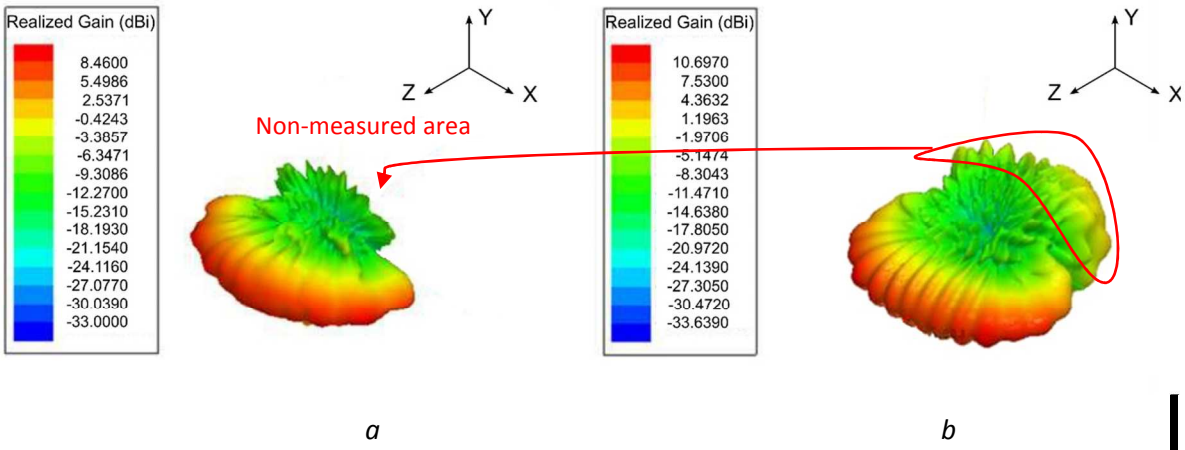

Fig. 12. 3D Radiation pattern for the realized gain of the copolar field component at 130 GHz.

a Measurements partial 3D pattern ($-40° < \theta < 90°$ and $0° < \phi < 360°$)
b Simulation complete 3D pattern

Please replace fig. 40 by 10 and 51 by 11 and 12.

Author's reply:

Thank you very much. The figure index has been corrected.

REVIEWER 2

The paper presents a novel integration solution at 130 GHz with fan-beamed antenna pattern and gain >5dBi. It is realized using a 3D printing lens. The solution is also low cost. The paper needs minor revision:

1) Fig. 40/ Fig. 50 Pls. revise the errors.

Author's reply:

Thank you very much. The figure index has been corrected.

2) It is claimed that the the 5 dBi is required with your link budget analysis. Pls. Provide a reference.

The 5dBi gain was calculated considering a transmitted power of 18 dBm and a RX sensitivity of -50 dBm, which are typical values for state of the art transceivers.

The link budget for the 3m line-of-sight F-band communication can thus be obtained as follows:

Sensitivity(dBm)=G_{tx}(dB)+G_{rx}(dB)+P_{tx}(dBm)-Propagation Losses(dB) -> -50= G_{tx}(dB)+G_{rx}(dB)+18 -83, yielding a gain value of 7.5 dBi in both extremes of the link, not the 5 dBi we stated and we apologize for our mistake in the calculation.

With this new value (7.5 dBi Gain in the extremes angles of the radiation pattern), the beamwidth of the H-plane of the proposed antenna is slightly reduced from 120° to 110°as can be seen in Fig 2 below, yielding a small modification in the initial scenario given in Fig.2 of the paper (Figure 3 below). In fact, the covered area of the sofa in the horizontal plane is now reduced to 8.5 m (initially 10m) which is still a "large" sofa.

References [1] and [2] together with the typical values employed in the link budget are now included in the revised version (see the modified sentence at the end of this answer). However, Figures 2 and 3 shown below have not been updated in the revised manuscript since we did not want to match our results with a new goal. However, if the reviewer agrees or asks for it, we could easily replace the two figures in the revised version 1 of the manuscript by those two new Figures below in a revised version number 2.

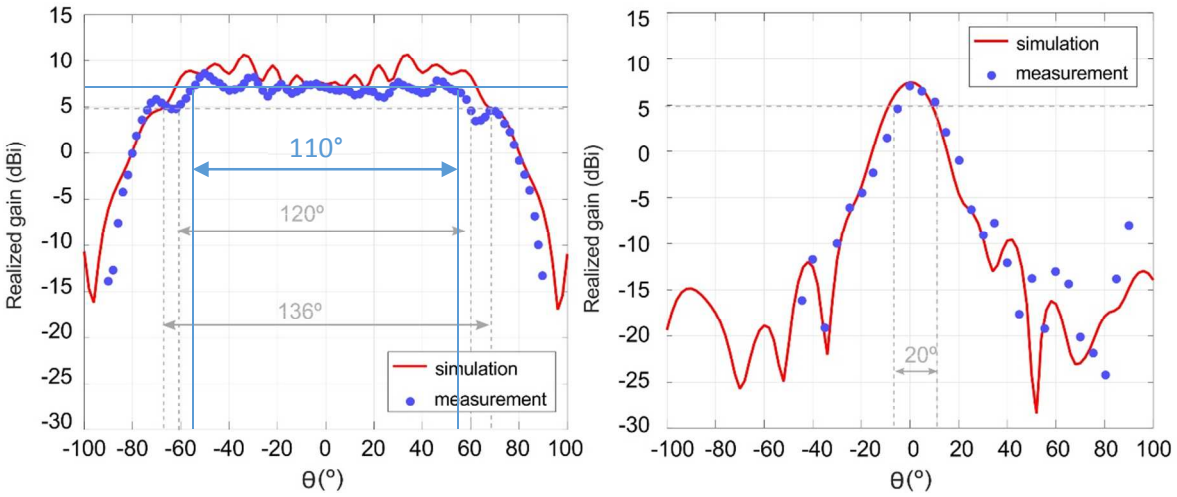

Figure 2 Main cuts of the radiation pattern. Left: H-plane, right: E-plane.

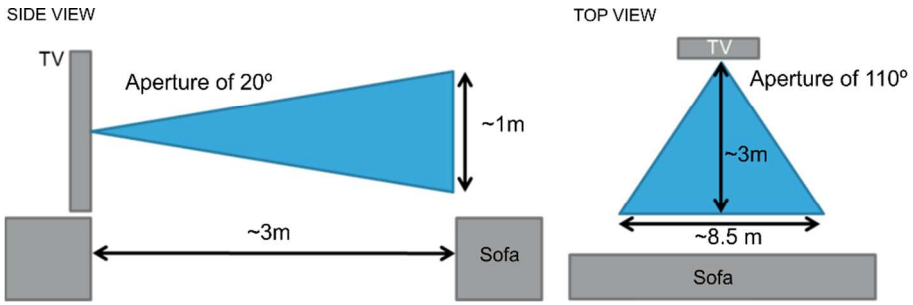

Figure 3. Modified scenario

[1] Z. Wang, P. Y. Chiang, P. Nazari, C. C. Wang, Z. Chen and P. Heydari, "A CMOS 210-GHz Fundamental Transceiver With OOK Modulation," in IEEE Journal of Solid-State Circuits, vol. 49, no.3, pp. 564-580, March 2014.

[2] N. Dolatsha, B. Grave, M. Sawaby, C. Chen, A. Babveyh, S. Kananian, A. Bisognin, C. Luxey, F. Gianesello, J. Costa, C. Fernandes, A. Arbabian, "A compact 130GHz fully packaged point-to-point wireless system with 3D-printed 26dBi lens antenna achieving 12.5Gb/s at 1.55pJ/b/m", IEEE International Solid-State Circuits Conference (ISSCC 2017), February 2017, San Francisco, USA.

MODIFIED TEXT IN THE MANUSCRIPT:

"For a LoS communication of 3 m in the F-band as the one described in ***Fig. 1***, and considering the radio performance of a typical transceiver with OOK modulation [17,18], 5dBi gain antennas are needed at both sides of the wireless link (typical values of 18 dBm transmitted power and -50 dBm sensitivity have been used for the link budget calculation)."